

Rb₄Mo₈P₁₂O₅₂, a Molybdenophosphate of the Cs₄Mo₈P₁₂O₅₂ Type: Structure and Properties of the Host Framework

D. RIOU AND M. GOREAUD

Laboratoire de Cristallographie et Sciences des Matériaux, CRISMAT, ISMRA, 14032 Caen Cedex, France

Received July 18, 1988; in revised form November 10, 1988

Green single crystals of Rb₄Mo₈P₁₂O₅₂ have been synthesized. They are monoclinic, space group *P*2₁, with *a* = 6.3847(9), *b* = 19,088(2), *c* = 9.7366(9) Å and β = 107.05(1)°, *Z* = 1. The structure, solved by the heavy-atom method was refined to *R* = 0.033 (*R*_w = 0.036) for 2237 reflections with σ(*I*)/*I* < 0.333. The framework, similar to that of Cs₄Mo₈P₁₂O₅₂ (K. H. Lii and Haushalter, *J. Solid State Chem.* **69**, 320 (1987)), presents two types of tunnels running along [100]. A systematic analysis of the voids and site potential calculations have shown the possibilities for insertion in the host framework. A pathway is obvious for medium-sized cations and ionic conduction is expected. © 1989 Academic Press, Inc.

Introduction

Molybdenophosphates present a large variety of structures among which tunnel structures seem to be the most numerous. TiMo₂P₃O₁₂ (1) and α-K₄Mo₈P₁₂O₅₂ (2) were described by Leclaire *et al.*, the latter structure being related to those of Cs₂Mo₄P₆O₂₆ and Cs₄Mo₈P₁₂O₅₂ reported recently by Lii and Haushalter (3). The framework of this oxide is particularly rich in voids, suggesting the existence of large possibilities for insertion. The present work deals with the structure of Rb₄Mo₈P₁₂O₅₂, compared to that of the Cs compound, and is completed by geometrical analysis of the framework and site potential calculations.

Experimental

Sample Preparation

Sparse single crystals of Rb₄Mo₈P₁₂O₅₂ were synthesized from mixtures of Rb₂CO₃,

(NH₄)₂HPO₄, and MoO₃ powders in appropriate ratios, first heated in a platinum crucible at 893 K to decompose the carbonate and phosphate. Then, the adequate amount of metallic Mo was added and, after grinding, the mixture was heated for 5 days at 1073 K in an evacuated silica ampoule. A green single crystal with the dimensions 36 × 48 × 96 μm without definite faces was chosen for X-ray diffraction investigation.

Structure Determination

Laue patterns suggest a monoclinic 2/*m* symmetry. The systematic conditions (0*k*0, *k* = 2*n*) for existence of the reflections obtained from Weissenberg and precession films led to the space group *P*2₁ or *P*2₁/*m*. The refinements show that the structure is acentric. The data were collected at 295 K on a CAD4 Enraf-Nonius diffractometer using the MoKα radiation (λ = 0.71069 Å) isolated by a graphite monochromator. An independent sector of the reciprocal lattice

TABLE I
POSITIONAL PARAMETERS WITH E.S.D.s FOR Rb₄Mo₈P₁₂O₃₂

	x	y	z	B (Å ²)
Rb(1)	0.2274(3)	0.160	0.0156(3)	3.92(4)
Rb(2)	0.7841(3)	0.4912(1)	0.3647(2)	2.85(3)
Mo(1)	0.1392(2)	0.49349(6)	0.0716(1)	0.49(1)
Mo(2)	0.5618(2)	0.03325(5)	0.3738(1)	0.44(1)
Mo(3)	0.6390(2)	0.31919(5)	0.0569(3)	0.49(1)
Mo(4)	0.9374(2)	0.28447(5)	0.6091(1)	0.53(1)
P(1)	0.0945(5)	0.3330(2)	0.9598(3)	0.57(5)
P(2)	0.7385(5)	0.1231(2)	0.6896(3)	0.51(5)
P(3)	0.5955(4)	0.4817(2)	0.9699(3)	0.59(5)
P(4)	0.7566(5)	0.1925(2)	0.2965(3)	0.55(5)
P(5)	0.0153(5)	0.0682(2)	0.2864(3)	0.64(5)
P(6)	0.4810(5)	0.2478(2)	0.6985(3)	0.55(5)
O(1)	0.881(1)	0.0303(4)	0.3690(8)	0.5(1)
O(2)	0.630(1)	0.2846(5)	0.6212(9)	1.1(1)
O(3)	0.941(1)	0.3058(4)	0.0397(8)	0.9(1)
O(4)	0.965(1)	0.0538(5)	0.1297(9)	1.3(1)
O(5)	0.254(1)	0.0590(4)	0.3719(9)	0.7(1)
O(6)	0.324(1)	0.3123(4)	0.0517(8)	0.8(1)
O(7)	0.900(1)	0.1731(4)	0.6591(8)	0.7(1)
O(8)	0.535(1)	0.2651(4)	0.8557(9)	0.9(1)
O(9)	0.244(1)	0.2570(4)	0.6112(9)	0.9(1)
O(10)	0.596(1)	0.1433(5)	0.3278(9)	1.0(1)
O(11)	0.047(1)	0.2941(5)	0.8178(8)	0.9(1)
O(12)	0.827(1)	0.2515(4)	0.4044(8)	0.7(1)
O(13)	0.445(1)	0.5004(5)	0.0617(8)	0.9(1)
O(14)	0.826(1)	0.0926(5)	0.8410(9)	1.1(1)
O(15)	0.587(1)	0.4056(5)	0.9283(9)	1.3(1)
O(16)	0.662(1)	0.0650(5)	0.5843(9)	1.2(1)
O(17)	0.672(1)	0.2225(4)	0.1476(8)	0.8(1)
O(18)	0.525(1)	0.1646(5)	0.6867(9)	1.0(1)
O(19)	0.977(1)	0.1501(4)	0.2977(8)	0.8(1)
O(20)	0.710(1)	0.3652(5)	0.2075(9)	1.4(2)
O(21)	0.069(1)	0.4123(4)	0.9335(8)	0.4(1)
O(22)	0.934(1)	0.3671(5)	0.5632(9)	1.1(1)
O(23)	0.203(1)	0.4468(5)	0.220(1)	1.3(1)
O(24)	0.464(1)	0.0296(5)	0.1611(9)	1.1(1)
O(25)	0.175(1)	0.0031(4)	0.9352(8)	0.8(1)
O(26)	0.449(1)	0.4494(5)	0.585(1)	1.5(2)

Anisotropic displacement parameters

	U(1, 1)	U(2, 2)	U(3, 3)	U(1, 2)	U(1, 3)	U(2, 3)
Rb(1)	0.0346(8)	0.0205(6)	0.071(1)	-0.0104(6)	-0.0207(8)	0.0123(7)
Rb(2)	0.0486(8)	0.0385(8)	0.0178(6)	0.0019(9)	0.0045(6)	-0.0103(7)
Mo(1)	0.0045(3)	0.0076(3)	0.0066(3)	0.0012(4)	0.0019(2)	-0.0001(4)
Mo(2)	0.0045(3)	0.0051(3)	0.0071(3)	-0.0005(4)	0.0017(3)	-0.0008(4)
Mo(3)	0.0053(3)	0.0069(3)	0.0063(3)	0.0012(4)	0.0014(3)	0.0008(4)
Mo(4)	0.0066(3)	0.0079(3)	0.0052(3)	-0.0003(4)	0.0010(3)	-0.0005(4)
P(1)	0.011(1)	0.001(1)	0.010(1)	-0.0014(9)	0.0035(9)	-0.002(1)
P(2)	0.007(1)	0.008(1)	0.004(1)	-0.000(1)	0.0014(9)	0.003(1)
P(3)	0.003(1)	0.015(1)	0.004(1)	-0.001(1)	0.0006(8)	0.002(1)
P(4)	0.007(1)	0.005(1)	0.009(1)	-0.003(1)	0.0018(9)	-0.004(1)
P(5)	0.008(1)	0.008(1)	0.009(1)	0.004(1)	0.0027(9)	0.001(1)
P(6)	0.006(1)	0.10(1)	0.006(1)	-0.003(1)	0.0025(9)	-0.002(1)

Note. $U_{ij} = \left(\frac{1}{2\pi^2}\right) \beta_{ij} a_i a_j (\text{Å}^2)$.

was registered in the range $-12 \leq h \leq 12$, $0 \leq k \leq 38$, $0 \leq l \leq 19$ with the ω - θ scanning mode, up to $\theta = 45^\circ$. A periodic control of the reflections 12 0 0, 0 38 0, and 0 0 19 has not shown any significant variation during the data collection. Among the 9870 measured reflections, only 2237 with $\sigma(I)/I < 0.333$ were corrected for Lorentz and polarization effects. The cell parameters of $\text{Rb}_4\text{Mo}_8\text{P}_{12}\text{O}_{52}$ were refined by least-squares from 25 reflections: $a = 6.3847(9)$, $b = 19.088(2)$, $c = 9.7366(9)$ Å, $\beta = 107.05(1)^\circ$, $Z = 1$. The crystal structure was solved by the heavy-atom method using the SDP programs (4). Rb and Mo atoms were located from the Patterson function and other atoms deduced in the subsequent difference synthesis. Scattering factors f , $\Delta f'$, and $\Delta f''$ were from "International Tables for X-Ray Crystallography" (12). Anisotropic thermal coefficients were refined for Rb, Mo, and P atoms and isotropic for oxygen atoms. No absorption correction has been applied due to the bad quality of the crystal facies. Atomic parameters were refined by full-ma-

trix least-squares in the $P2_1$ space group, up to $R = 0.033$ and $R_w = 0.036$ (Table I).

Description of the Structure and Discussion

The molybdenophosphate $\text{Rb}_4\text{Mo}_8\text{P}_{12}\text{O}_{52}$ presents a mixed framework built up from corner-sharing $[\text{MoO}_6]$ octahedra and $[\text{PO}_4]$ tetrahedra (Figs. 1 and 2). The cell contains six independent phosphorus atoms: each P(1) and P(3) atom is linked with four $[\text{MoO}_6]$ octahedra whereas P(2), P(6) and P(4), P(5) are paired to form two diphosphate groups. The single $[\text{PO}_4]$ groups are quite regular with a mean P–O bond 1.525 Å (Table II). The $[\text{P}_2\text{O}_7]$ units show, as in other diphosphates, a long P–O bond (from 1.57 to 1.62 Å) between P and the O-bridging atom in $[\text{P}_2\text{O}_7]$ and three shorter bonds (from 1.49 to 1.54 Å) with the terminal oxygen atoms (Table II). The diphosphate groups are in a nearly eclipsed conformation. The values of P(2)–O(18)–P(6) and P(4)–O(19)–P(5) angles are $131.1(8)^\circ$ and

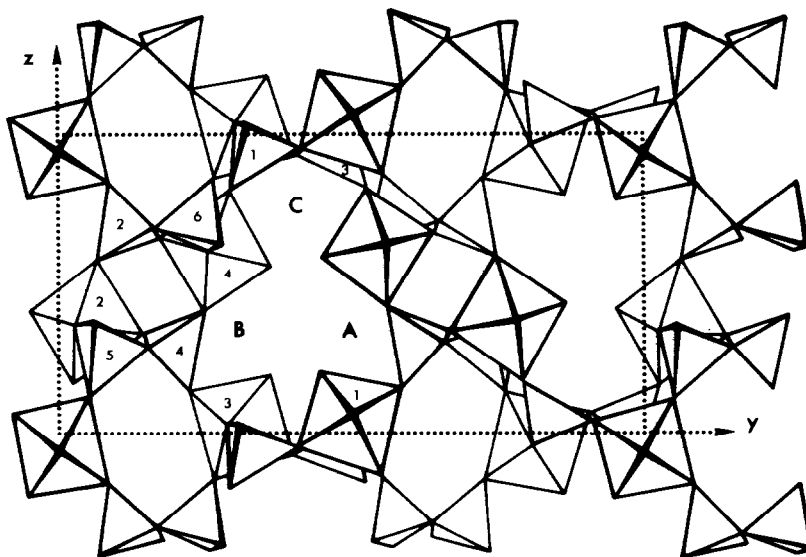


FIG. 1. $\text{Rb}_4\text{Mo}_8\text{P}_{12}\text{O}_{52}$: Polyhedron representation of the structure along $[100]$. Numbers refer to Mo and P atoms of Table I.

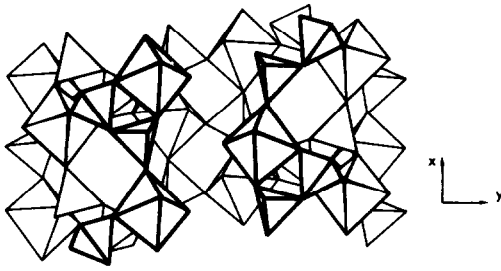


FIG. 2. $\text{Rb}_4\text{Mo}_8\text{P}_{12}\text{O}_{52}$: Partial representation of the structure along [001].

TABLE II
INTERATOMIC DISTANCES IN ANGSTROMS
IN $\text{Rb}_4\text{Mo}_8\text{P}_{12}\text{O}_{52}$

Rb(1)–O(14)	2.93(1)	Rb(2)–O(20)	2.82(1)
–O(6)	2.97(1)	–O(1)	2.93(1)
–O(17)	3.00(1)	–O(5)	2.95(1)
–O(4)	3.04(1)	–O(25)	3.02(1)
–O(24)	3.04(1)	–O(22)	3.03(1)
–O(25)	3.09(1)	–O(13)	3.11(1)
–O(11)	3.20(1)	–O(16)	3.34(1)
–O(10)	3.27(1)		
–O(3)	3.37(1)		
Mo(1)–O(23)	1.65(1)	Mo(3)–O(20)	1.65(1)
–O(13)	1.99(1)	–O(3)	2.00(1)
–O(25)	2.00(1)	–O(6)	2.00(1)
–O(21)	2.01(1)	–O(17)	2.03(1)
–O(14)	2.06(1)	–O(15)	2.04(1)
–O(4)	2.20(1)	–O(8)	2.14(1)
Mo(2)–O(26)	1.66(1)	Mo(4)–O(22)	1.64(1)
–O(24)	1.98(1)	–O(11)	1.954(9)
–O(5)	2.02(1)	–O(2)	2.00(1)
–O(1)	2.05(1)	–O(12)	2.01(1)
–O(16)	2.05(1)	–O(9)	2.02(1)
–O(10)	2.17(1)	–O(7)	2.21(1)
P(1)–O(3)	1.51(1)	P(4)–O(10)	1.49(1)
–O(11)	1.52(1)	–O(17)	1.50(1)
–O(6)	1.53(1)	–O(12)	1.52(1)
–O(21)	1.54(1)	–O(19)	1.62(1)
P(2)–O(16)	1.49(1)	P(5)–O(4)	1.49(1)
–O(7)	1.50(1)	–O(1)	1.52(1)
–O(14)	1.53(1)	–O(5)	1.52(1)
–O(18)	1.57(1)	–O(19)	1.59(1)
P(3)–O(15)	1.51(1)	P(6)–O(8)	1.50(1)
–O(24)	1.52(1)	–O(9)	1.51(1)
–O(13)	1.53(1)	–O(2)	1.54(1)
–O(25)	1.54(1)	–O(18)	1.62(1)

129.8(8)°, respectively, very close to the value 132.86(9)° observed in NaFeP_2O_7 (5) in which $[\text{P}_2\text{O}_7]$ has the same conformation. In KFeP_2O_7 (6), which exhibits a staggered conformation for $[\text{P}_2\text{O}_7]$, the P–O–P angle is only 124.3(1)°. The environment of the two independent $[\text{P}_2\text{O}_7]$ groups is identical: each of them shares four apices with four $[\text{MoO}_6]$ octahedra and two apices with the same octahedra, then forming a $[\text{MoP}_2\text{O}_{11}]$ unit similar to the $[\text{FeP}_2\text{O}_{11}]$ unit in NaFeP_2O_7 (5).

The coordination of the molybdenum atoms in this structure is typical of the Mo behavior: as in $\alpha\text{-K}_4\text{Mo}_8\text{P}_{12}\text{O}_{52}$ (2) or $\text{Cs}_2\text{Mo}_4\text{P}_6\text{O}_{26}$ (3), four coplanar neighbors lie at the mean distance 2.01 Å, one is very close (mean $d = 1.65$ Å), and another is farther (2.18 Å). Every independent so-formed $[\text{MoO}_6]$ irregular octahedron presents a free O-apex lying at the boundary of a tunnel of the framework. The shortest Mo–O distance corresponds precisely to this free apex. If we consider their environment, the $[\text{MoO}_6]$ octahedra fall into two categories characterized by a different distribution of the connections with the $[\text{PO}_4]$ and $[\text{P}_2\text{O}_7]$ units (Table III), e.g., Mo(1) and Mo(3) do not form $[\text{MoP}_2\text{O}_{11}]$ rings with the diphosphate groups.

The framework shows two sorts of tunnels parallel with the [100] direction (Fig. 1). The first type has a section with a complex shape and could be described as the

TABLE III
ENVIRONMENT OF THE $[\text{MoO}_6]$ OCTAHEDRA

Octahedron	Single $[\text{PO}_4]$	$[\text{P}_2\text{O}_7]$ groups	$[\text{P}_2\text{O}_7]$ forming	Free O atoms
			$[\text{MoP}_2\text{O}_{11}]$ groups	
$[\text{Mo}(1)\text{O}_6]$	3	2	0	1
$[\text{Mo}(2)\text{O}_6]$	1	2	1	1
$[\text{Mo}(3)\text{O}_6]$	3	2	0	1
$[\text{Mo}(4)\text{O}_6]$	1	2	1	1

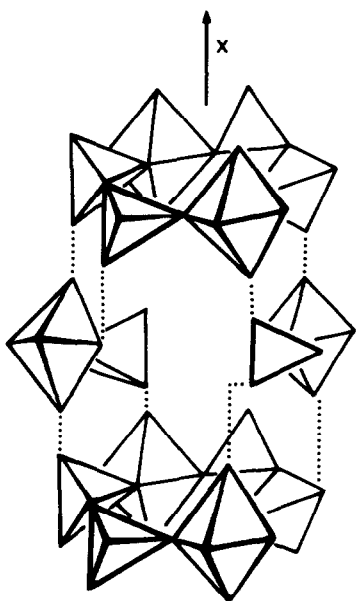


FIG. 3. Schema of a cage forming the hexagonal [100] tunnels, built up from two $[\text{Mo}_2\text{P}_4\text{O}_{22}]$ rings and two opposite $[\text{MoPO}_9]$ units.

result of the junction of three narrow channels (A, B, and C on Fig. 1), involving the existence of unsaturated oxygen atoms at the periphery of the tunnel. The resulting tunnel is defined by noncoplanar rings of five octahedra and five tetrahedra linked together in an alternate disposition. The tunnels of the second type present a hexagonal section due to rings that extend roughly in the (100) plane. These rings are built up from two opposite $[\text{Mo}(1)\text{O}_6]$ and $[\text{Mo}(3)\text{O}_6]$ octahedra and two opposite $[\text{P}_2\text{O}_7]$ groups (Fig. 3). The resulting $[\text{Mo}_2\text{P}_4\text{O}_{22}]$ rings are stacked along the [100] direction and joined through two opposite $[\text{MoPO}_9]$ units (one $[\text{MoO}_6]$ linked to a single $[\text{PO}_4]$). Then a group of two rings and two $[\text{MoPO}_9]$ units define a cage which communicates with tunnels of the first type (Fig. 3). Tunnels of the second type result from the succession of such cages along [100]. One can note the existence of rings forming tunnels in $\text{P}_8\text{W}_{12}\text{O}_{52}$ (7) (Fig. 4a) but

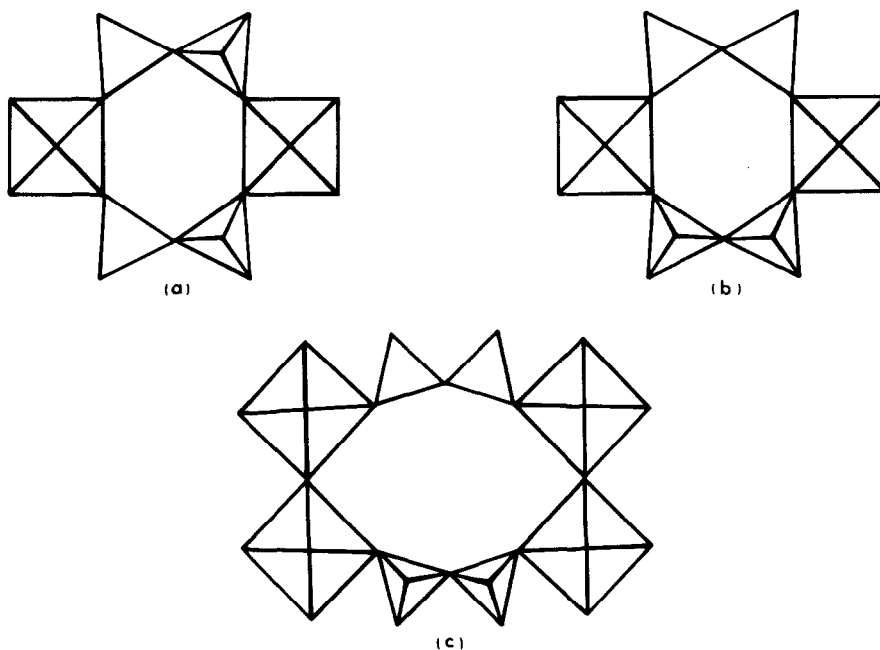


FIG. 4. Schematic representation of rings forming tunnels in (a) $\text{P}_8\text{W}_{12}\text{O}_{52}$, (b) $\text{Rb}_4\text{Mo}_8\text{P}_{12}\text{O}_{52}$, (c) $\text{CsP}_8\text{W}_8\text{O}_{40}$.

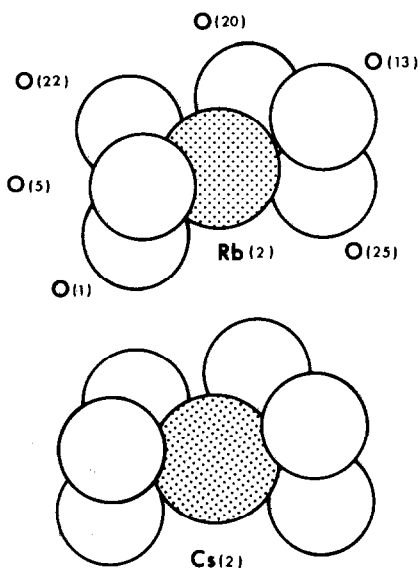


FIG. 5. Coordination of Rb^+ and Cs^+ in site (2) of the $[\text{Mo}_8\text{P}_{12}\text{O}_{52}]$ framework.

they differ by the conformation of the $[\text{P}_2\text{O}_7]$ units which are staggered and not eclipsed as in $\text{Rb}_4\text{Mo}_8\text{P}_{12}\text{O}_{52}$ (Fig. 4b). In $\text{CsP}_8\text{W}_8\text{O}_{40}$ (8) the configuration is eclipsed but the rings are octagonal (Fig. 4c) and formed by four octahedra and two diphosphate units.

The coordination of Rb^+ and Cs^+ in the $[\text{Mo}_8\text{P}_{12}\text{O}_{52}]$ framework is not regular as shown in Figs. 5 and 6, the oxygen neighbors being distributed on opposite poles of the alkaline ion. It is worth noting that $\text{Rb}(2)$ and $\text{Cs}(2)$ have strictly the same behavior. For $\text{Rb}(1)$ and $\text{Cs}(1)$, lying in the hexagonal tunnels, the only difference is a seventh oxygen close neighbor for Cs^+ which is relatively farther off in the case of Rb^+ (Table II).

The research into insertion possibilities of the $[\text{Mo}_8\text{P}_{12}\text{O}_{52}]$ framework has been made by means of systematic geometrical analysis and site potential calculations. During a first search, 18,000 points were tested in the independent volume of the cell with a step of about 0.33 \AA in order to locate domains of possible insertion in terms

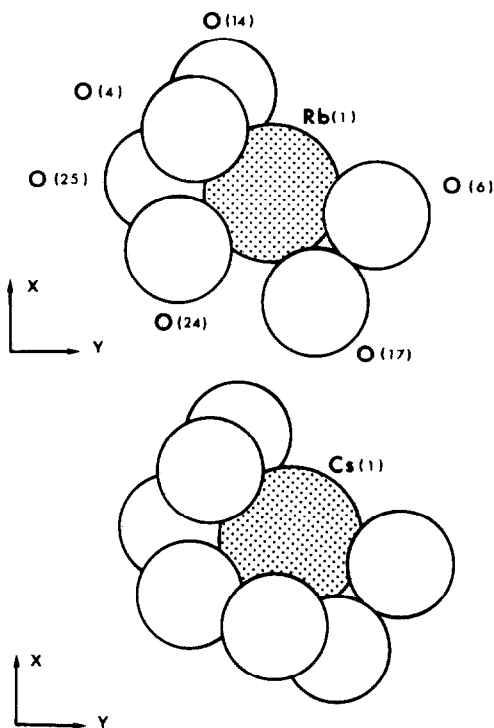


FIG. 6. Coordination of Rb^+ and Cs^+ in site (1) of the $[\text{Mo}_8\text{P}_{12}\text{O}_{52}]$ framework.

of ionic radii. A better delimitation was obtained with a step of about 0.06 \AA . For each solution a coordination diagram can be produced by the program COORD (9). Site potentials were calculated by an adaptation of the program published by Jacoboni (10) and based on the Bertaut method (11). The covalent character of the P–O bonds were taken into account and results are in $\text{e}\text{\AA}^{-1}$.

The energy calculated for the actual positions of $\text{Rb}(1)$ is $-0.51 \text{ e}\text{\AA}^{-1}$ and for $\text{Rb}(2)$ is $-0.95 \text{ e}\text{\AA}^{-1}$. These values suggest, in the case of a partial occupation, that the hexagonal tunnels would be filled only after the $\text{Rb}(2)$ sites were filled (A in Fig. 1). The B sites are not equivalent to A sites: the energy around the B positions is $-0.70 \pm 0.08 \text{ e}\text{\AA}^{-1}$. On C sites, corresponding roughly to the position 0.20 0.41 0.75, we find $-0.72 \text{ e}\text{\AA}^{-1}$. All these values are favorable to insertion of alkaline ions, but the geometrical

TABLE IV
EXTENSION OF DOMAINS OF INSERTION FOR A IONS
AS Cs⁺ GIVING A-O DISTANCES ABOVE 2.9 Å

Site	Rb ₄ Mo ₈ P ₁₂ O ₅₂ framework	Cs ₄ Mo ₈ P ₁₂ O ₅₂ framework
(1)	$x = 0.25 \pm 0.05$	$x = 0.73 \pm 0.01$
	$y = 0.159 \pm 0.006$	$y = 0.913 \pm 0.004$
	$z = -0.015 \pm 0.067$	$z = 0.004 \pm 0.008$
(2)	$x = 0.768 \pm 0.02$	$x = 0.715 \pm 0.008$
	$y = 0.505 \pm 0.005$	$y = 0.748 \pm 0.003$
	$z = 0.355 \pm 0.005$	$z = 0.636 \pm 0.009$

Note. Values are the limits of x , y , and z observed for the position of the center of A ions. The shape of a domain is roughly an ellipsoid.

analysis shows that the C position is unsuitable for Rb⁺ (or Cs⁺), some Rb-O distances being too short.

With the condition $A^+-O > 2.9$ Å, the geometrical analysis shows a very poor extension for the domains of possible insertion of big A⁺ cations. The values reported in Table IV show more voluminous favorable domains for the center of Cs⁺ ions in the Rb₄Mo₈P₁₂O₅₂ than in the Cs₄Mo₈P₁₂O₅₂ framework: in fact, due to the difference of ionic radii, the effective volumes of the domains are almost the same for Rb⁺ and Cs⁺ in both frameworks. The results for ions of

TABLE V
EXTENSION OF DOMAINS OF INSERTION FOR Rb⁺
AND K⁺ IONS IN THE Rb₄Mo₈P₁₂O₅₂ FRAMEWORK

Site	Rb ⁺	K ⁺
(1)	$x = 0.26 \pm 0.10$	$x = 0.25 \pm 0.15$
	$y = 0.15 \pm 0.02$	$y = 0.15 \pm 0.02$
	$z = 0.00 \pm 0.10$	$z = -0.02 \pm 0.12$
(2A)	$x = 0.76 \pm 0.08$	$x = 0.75 \pm 0.15$
	$y = 0.52 \pm 0.04$	$y = 0.52 \pm 0.04$
	$z = 0.35 \pm 0.04$	$z = 0.37 \pm 0.03$
(2B)	$x = 0.29 \pm 0.08$	$x = 0.29 \pm 0.13$
	$y = 0.29 \pm 0.03$	$y = 0.29 \pm 0.05$
	$z = 0.33 \pm 0.02$	$z = 0.34 \pm 0.04$

Note. Values are for the center of ions and distances are above 2.7 Å for Rb-O and 2.6 Å for K-O.

medium or small size confirm that the C position is unsuitable for insertion. For the (1) and (2) sites and A/B positions, the possibilities are given in Table V.

For ions with the size of Na⁺, geometrical and potential calculations show the existence of a pathway characterized by favorable values of the energy and coordination states similar to that usually observed for Na⁺ (Fig. 7). So, the [Mo₈P₁₂O₅₂] framework may be ionic conducting. Geometrical investigations for small ions as Li⁺ give poor results: only some positions are possible for insertion, leading to a pseudotetrahedral coordination with O atoms.

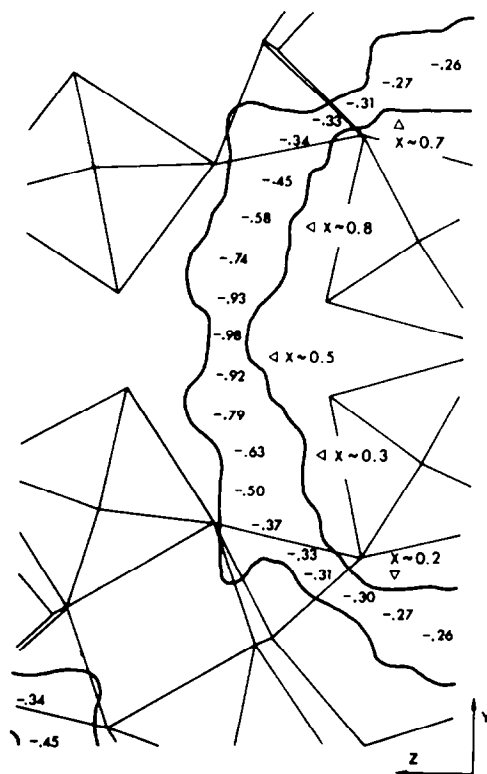


FIG. 7. Pathway for cations with a radius of 1 Å, in the [Mo₈P₁₂O₅₂] framework. Curves are limits for the position of the center of a hypothetical cation. The values of site energy are given in eV⁻¹ for a univalent cation lying at middle height in the pathway, the thickness of which varies from about 0.7 to 3 Å.

Conclusion

The frameworks of the compounds $\text{Cs}_4\text{Mo}_8\text{P}_{12}\text{O}_{52}$ (3) and $\text{Rb}_4\text{Mo}_8\text{P}_{12}\text{O}_{52}$ are almost identical and because the difference between the ionic radii of Rb^+ and Cs^+ is partially balanced by the adaptation of cell dimensions, the behaviors of Rb^+ and Cs^+ in these structures are almost the same. Systematic geometrical and potential calculations have shown the existence of a pathway in the framework for ions of medium size as Na^+ . Therefore, ionic conduction properties can be expected for that type of compound.

Acknowledgments

We are grateful to Mrs. Josiane Chardon for help with the X-ray diffraction.

References

1. A. LECLAIRE, J. C. MONIER, AND B. RAVEAU, *J. Solid State Chem.* **59**, 301 (1985).
2. A. LECLAIRE, J. C. MONIER, AND B. RAVEAU, *J. Solid State Chem.* **48**, 147 (1983).
3. K. H. LIU AND R. C. HAUSHALTER, *J. Solid State Chem.* **69**, 320 (1987).
4. B. A. FRENZ AND ASSOCIATES, INC., College Station, TX 77840 and Enraf-Nonius, Delft (1985).
5. M. GABELICA-ROBERT, M. GOREAUD, PH. LABBE, AND B. RAVEAU, *J. Solid State Chem.* **45**, 389 (1982).
6. D. RIOU, PH. LABBE, AND M. GOREAUD, *Eur. J. Solid State Inorg. Chem.* **25**, 215 (1988).
7. B. DOMENGES, M. GOREAUD, PH. LABBE, AND B. RAVEAU, *Acta Crystallogr. Sect. B* **38**, 1724 (1982).
8. M. GOREAUD, PH. LABBE, AND B. RAVEAU, *J. Solid State Chem.* **56**, 41 (1985).
9. M. GOREAUD, unpublished.
10. C. JACOBONI, *Thèse, Paris VI* (1976).
11. E. F. BERTAUT, *J. Phys. Radium* **13**, 499 (1952).
12. "International Tables for X-Ray Crystallography," Kynoch Press, Birmingham (1974).